Supporting Information

Organic Redox Additive Incorporated PANI Hydrogel Electrodes for Flexible High-Energy-Density Supercapacitors

*Liyang Dou[a], Shixiang Zhou[b], Jie Ma[a], Cheng Zhao[a], Peixin Cui[a], Shifang Ye[a], Peizhong Feng[a], Xiuquan Gu[a], Sheng Huang[a], Xueyu Tao[a]**

[a] School of Materials and Physics, China University of Mining and Technology, Xuzhou 221116, Jiangsu, China.

[b] Department of Materials Science and Engineering, National University of Singapore, 117575, Singapore.

* Corresponding author.

Email address: taoxueyu@cumt.edu.cn.

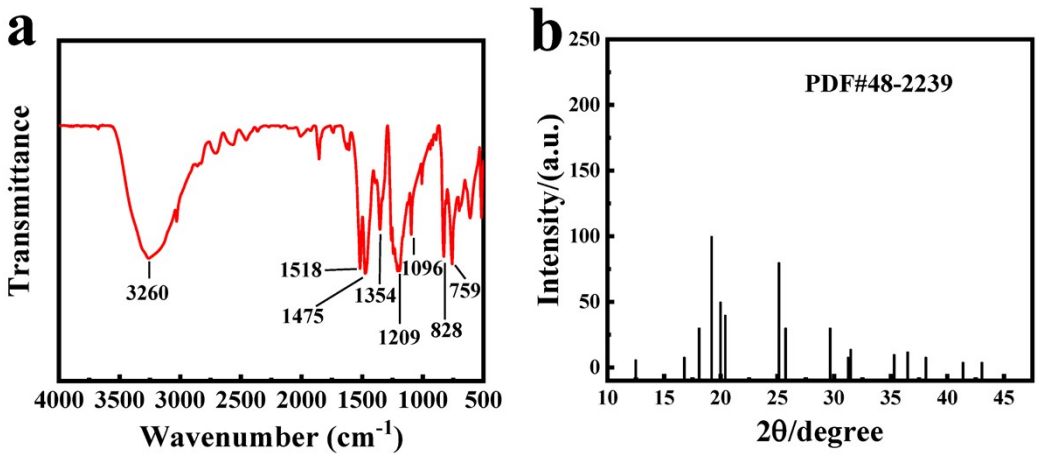

Fig. S1. (a) FTIR spectrum and (b) XRD of HQ.

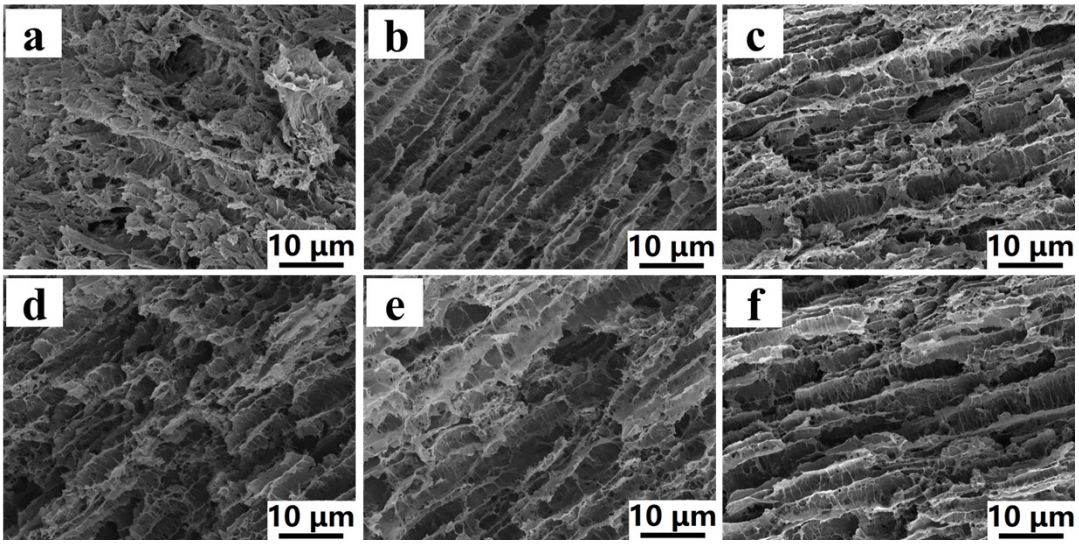

Fig. S2. SEM images from another cross-section that was perpendicular to the 3D porous-like cross-section: (a) PP hydrogel; (b-f) PHP hydrogels with various concentrations of HQ: 5, 10, 15, 20, 25 mmol/L.

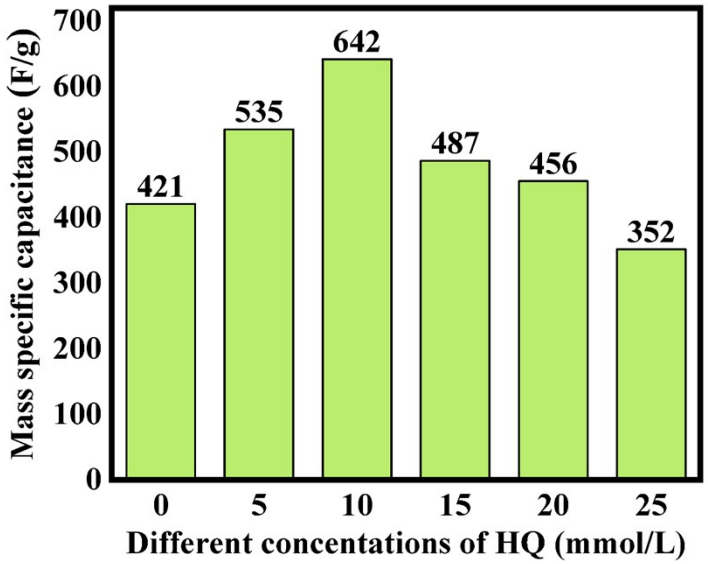

Fig. S3. Specific capacitance of PHP hydrogel electrodes with various concentrations of HQ at current density of 0.5 A/g.

Table S1. Specific capacitance of PHP hydrogel electrodes at different scan rates.

Scan rate (mV/s)	PP	PHP-5	PHP-10	PHP-15	PHP-20	PHP-25
5	424	487	591	549	546	542
10	386	420	535	506	502	493
20	323	362	457	441	436	430
30	260	304	403	392	390	386
50	209	251	330	315	308	302
100	136	176	230	209	203	195

Table S2. Specific capacitance of PHP hydrogel electrodes at different current densities.

Current density (A/g)	PP	PHP-5	PHP-10	PHP-15	PHP-20	PHP-25
0.5	421	535	642	487	475	456
1.0	359	444	512	394	385	379
1.5	339	392	441	368	357	352
2.5	320	339	369	346	341	336
5.0	289	291	325	320	318	312

Table S3. Resistance of PP and PHP hydrogel electrodes.

Resistance	PP	PHP-5	PHP-10	PHP-15	PHP-20	PHP-25
R_{ct}	0.81	0.31	0.28	0.29	0.30	0.32
R_s	2.06	1.38	1.01	1.20	1.62	1.68

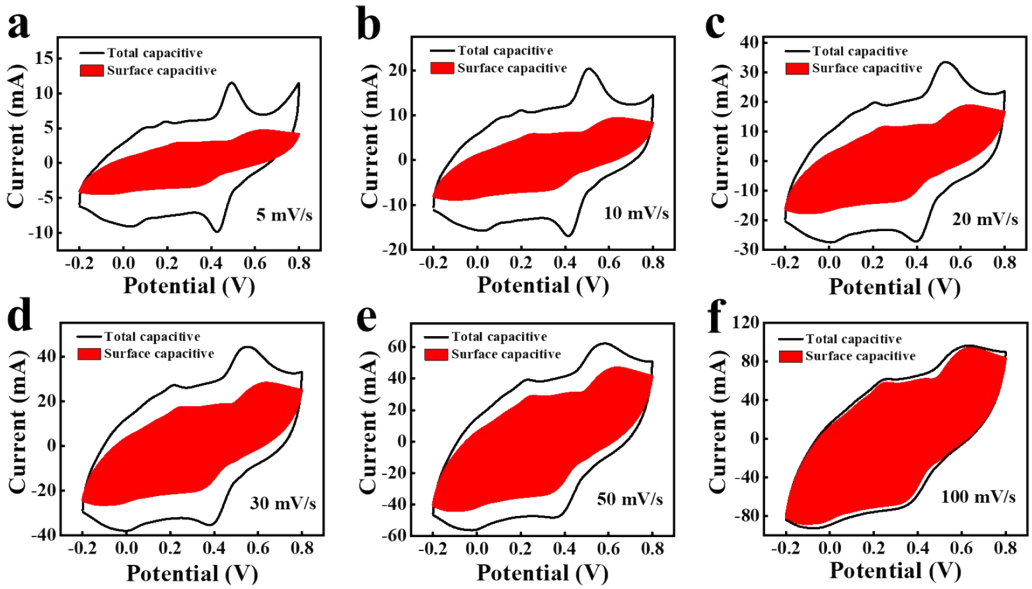

Fig. S4. Cyclic voltammetry of PHP-10 hydrogel electrode measured at different scan rates: (a) 5 mV/s, (b) 10 mV/s, (c) 20 mV/s, (d) 30 mV/s, (e) 50 mV/s, (f) 100 mV/s. The shadowed area is the capacitive contribution.

Table S4. The diffusion-controlled and surface capacitive of PHP hydrogel electrodes at different scan rates.

Scan rate (mV/s)	PP		PHP-5		PHP-10		PHP-15		PHP-20		PHP-25	
	C_s	C_d	C_s	C_d	C_s	C_d	C_s	C_d	C_s	C_d	C_s	C_d
5	127	297	163	324	202	389	193	356	188	358	173	369
10	127	259	163	257	202	334	193	313	188	314	173	320
20	127	196	163	199	202	255	193	248	188	248	173	257
30	127	133	163	141	202	202	193	199	188	202	173	213
50	127	82	163	88	202	127	193	122	188	120	173	129
100	127	9	163	13	202	27	193	16	188	15	173	22

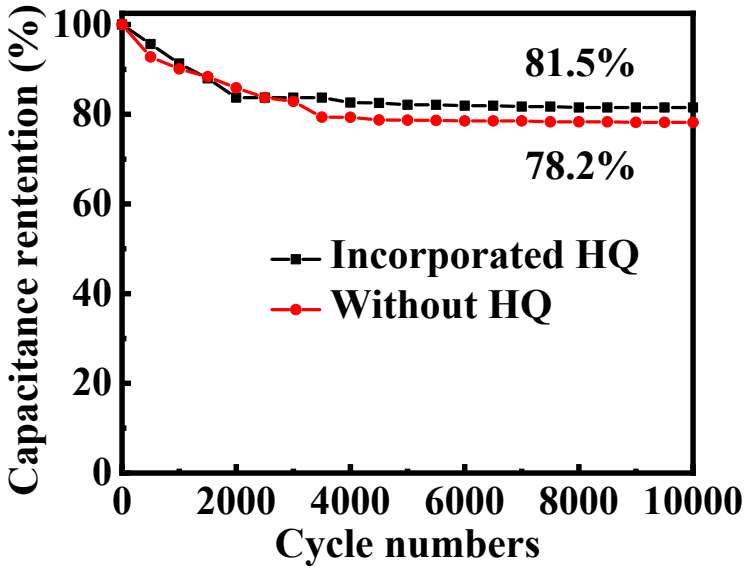

Fig. S5. Cycle stability of PANI hydrogel electrodes with and without HQ at 1.5 A/g current density.

It can be seen from the SEM before and after cycling, the morphology of PHP-10 hydrogel electrode and PVA/H_2SO_4 gel electrolyte had changed (Fig. S6). Firstly, the PHP-10 hydrogel electrode exhibited a honeycomb-like three-dimensional network structure with uniform pore size distribution and thin pore walls before the cycle (Fig. S6a). After 10,000 discharge/charge cycles, the morphology of the hydrogel electrode surface became rougher and displayed obvious loose pore walls, indicating that dissolution or other side reactions had occurred during the cycling process, and thus the repeated cycling could deteriorate the electrode structure (Fig. S6b). Secondly, the PVA/H_2SO_4 gel electrolyte had a three-dimensional network structure with regular and uniform pore sizes, while after 10,000 cycles, the pore walls of the hydrogel became thicker and the pores shrank, which may be due to the entanglement of polymer chains

(Fig. S6c, d).

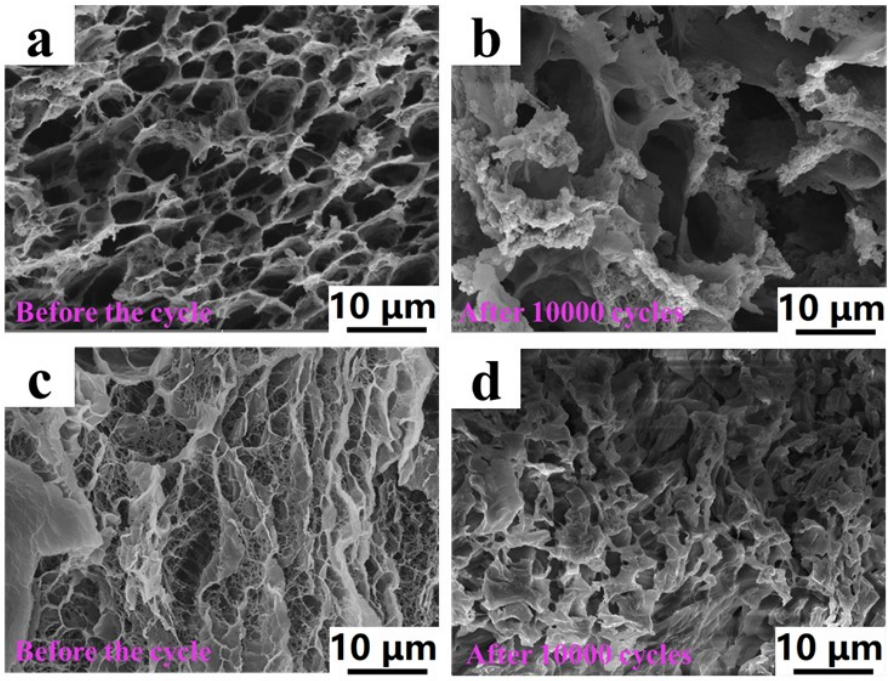

Fig. S6. SEM images of (a-b) PHP-10 hydrogel and (c-d) PVA/H_2SO_4 gel electrolyte before and after 10,000 charge/discharge cycles.

The electrochemical tests of the PHP-10 hydrogel electrode before and after cycling were shown in Fig. S7. The electrochemical performance decreased after 10,000 charge/discharge cycles. The CV, GCD, EIS, and cycle stability data of PHP-10 hydrogel electrode were performed in an asymmetric three-electrode cell setup using 1 M H_2SO_4 as an electrolyte in the fixed potential window of -0.2 to 0.8 V. It can be seen from CV curves (Fig. S7a) that after 10,000 charge/discharge cycles, the peak of CV curves of PHP-10 hydrogel electrode did not change, only the integrated area became smaller than that of before the cycle, revealing its capacitive response became worse ($C_m = \frac{\int Idv}{2 * Sr * m * \Delta U}$). GCD result (Figure S7b) showed the symmetrical charge-discharge curves of the electrode remained the same after cycling study. It can

be observed from the GCD curves that PHP-10 hydrogel electrode took less time to complete a charge/discharge cycle after 10,000 cycles than before the cycle. It can be found that the calculated specific capacitance at current density of 0.5 A/g was 603 F/g ($C_m = \frac{I\Delta t}{m\Delta U}$), which was lower than that of before the cycle (642 F/g). EIS curves (Figure S7c) implied that the R_s and R_{ct} values of PHP-10 hydrogel electrode were 1.23 Ω and 3.98 Ω, which were both higher than that of before the cycle (0.71 Ω and 1.35 Ω). Besides, the electrode exhibited superior cycling stability with a capacitance retention of 81.5% in 10,000 charge/discharge cycles (Figure S7d). Thus, the electrochemical performance of PHP-10 hydrogel electrode did decrease after 10,000 charge/discharge cycles.

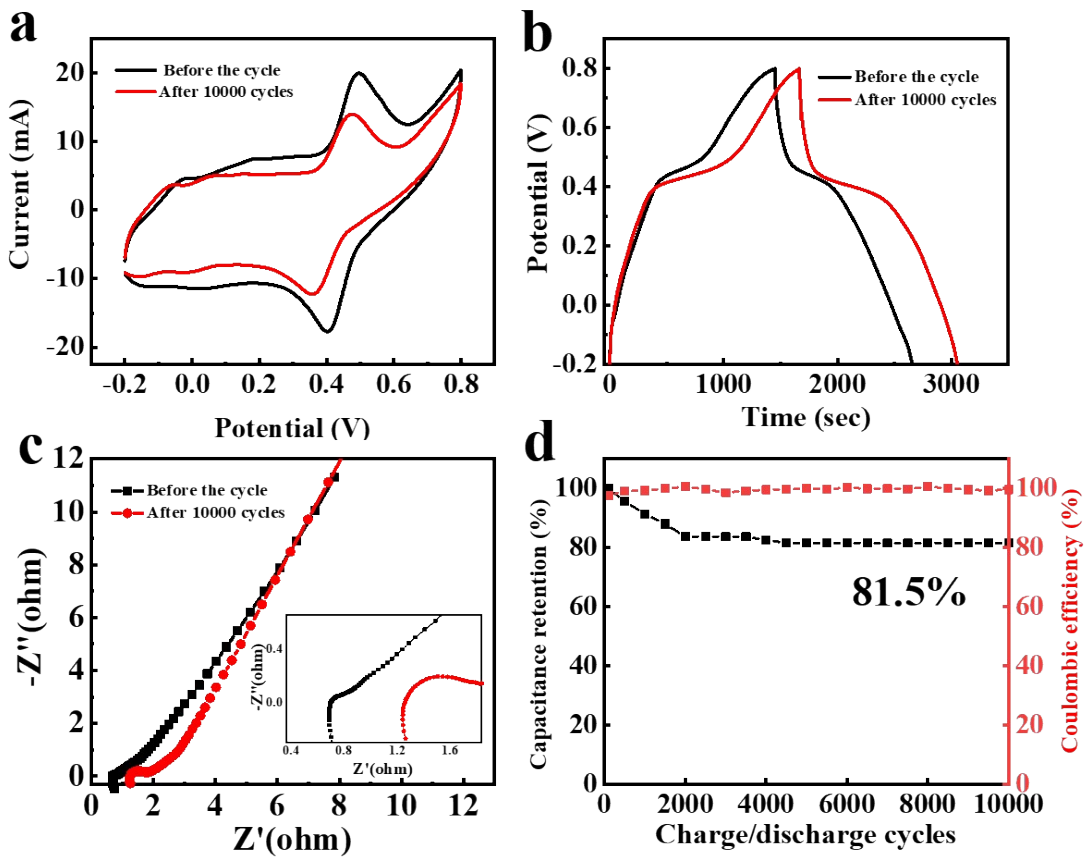

Fig. S7. Electrochemical performance of PHP-10 hydrogel electrode before and after

10,000 charge/discharge cycles: (a) CV curves under scan rate of 5 mV/s; (b) GCD curves at current density of 0.5 A/g; (c) Nyquist plots; (d) Cycle stability at 1.5 A/g current density.

The electrochemical tests of the supercapacitor based on PHP-10 hydrogel electrodes and PVA/H_2SO_4 gel electrolyte before and after 10,000 charge/discharge cycles were shown in Fig. S8. The electrochemical performance decreased after 10,000 charge/discharge cycles. It can be seen from CV, Ragone plot, and EIS curves (Fig. S8a-c) that after 10,000 charge/discharge cycles, the supercapacitor had a smaller integrated area of CV curve than that of before the cycle. The calculated energy density was 8.5 Wh/kg at the power density of 125 W/kg, which was lower than that of before the cycle (energy density of 12.5 Wh/kg at the power density of 125 W/kg). The internal resistance increased and the capacitive performance decreased. Besides, the supercapacitor exhibited cycling stability with a capacitance retention of 77.6 % in 10,000 charge/discharge cycles (Fig. S8d). Therefore, the electrochemical performance of the supercapacitor did decrease after 10,000 charge/discharge cycles.

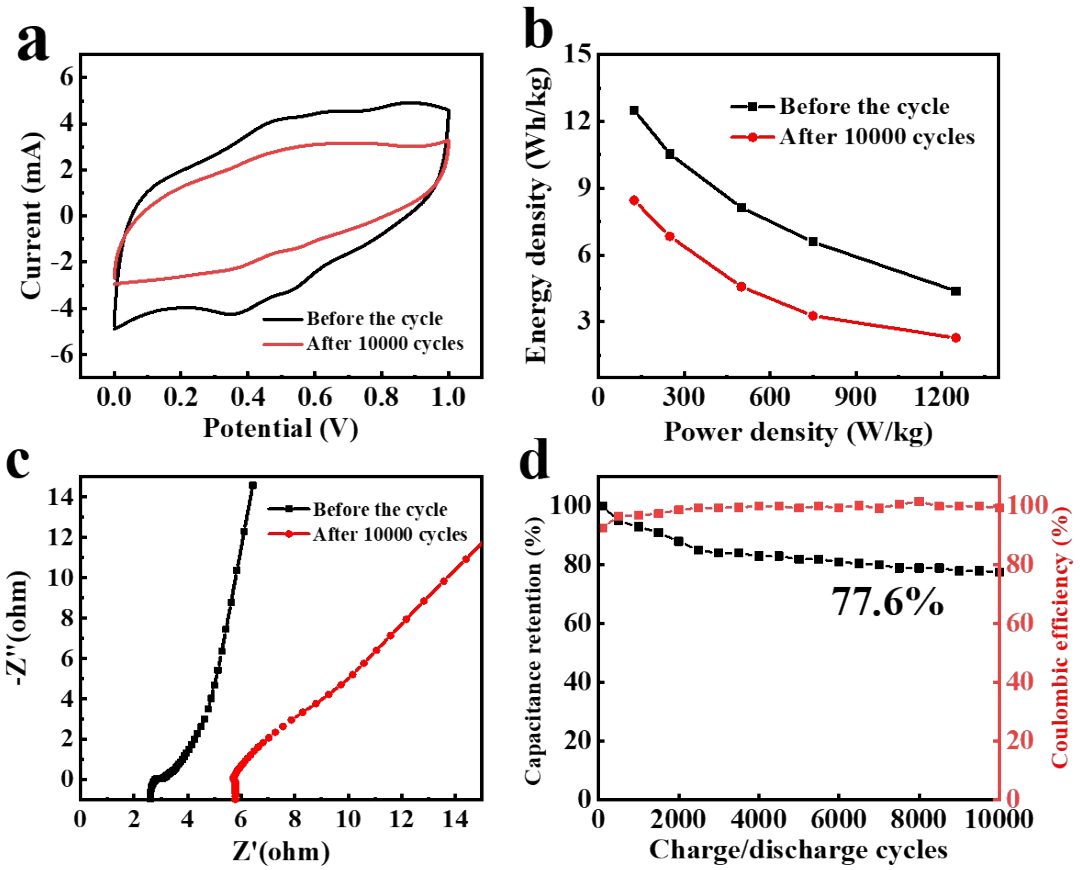

Fig. S8. Electrochemical performance of flexible supercapacitor based on PHP-10 hydrogel electrodes and PVA/H_2SO_4 gel electrolyte before and after 10,000 charge/discharge cycles: (a) CV curves at 10 mV/s scan rate; (b) Ragone plots; (c) Nyquist plots; (d) Cycle stability at 1.5 A/g current density.

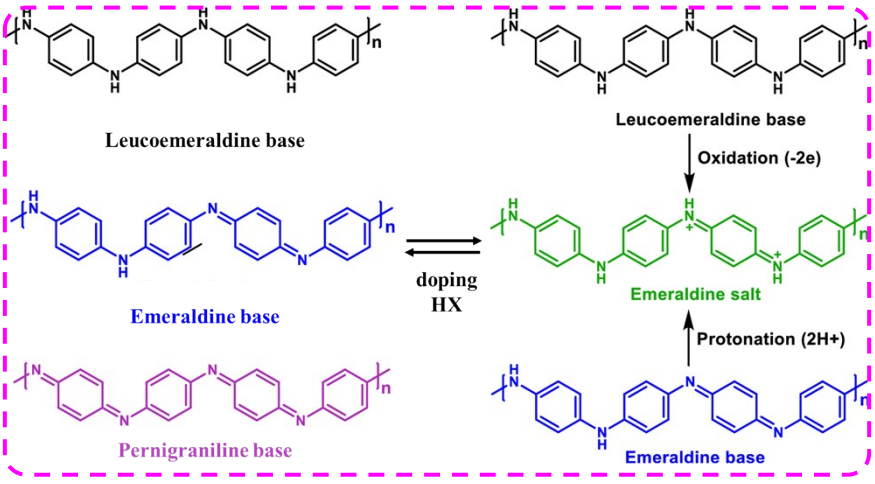

Fig. S9. Different forms and oxidation/protonation transition processes of

polyaniline [1].

Table S5. Comparison of electrochemical performance of supercapacitors based on PANI electrodes.

Electrode materials	Energy density	Power density	Cycle stability	Ref.
PANI/PVA	7.8 Wh/kg	200 W/kg	87% (3,000)	2
PANI/PVA/TiO_2	2.8 Wh/kg	125.0 W/kg	86.9% (10)	3
PANI/CNT/PVA	14.3 μWh/cm^2	97.5 μW/cm^2	87.5% (1,000)	4
PANI/PyHCP	0.57 Wh/kg	320.63 W/kg	90.7% (2,000)	5
PANI/PVA	49.9 μWh/cm^2	0.4 mW/cm^2	76% (10,000)	6
PANI/CF	2.5 Wh/kg	300 W/kg	86.1% (1,000)	7
PANI/HQ/PVA	12 Wh/kg	125 W/kg	77.6% (10,000)	This work

Fig. S10. Digital photo of PHP-10 hydrogel-based FSCs wrapped with VPH film.

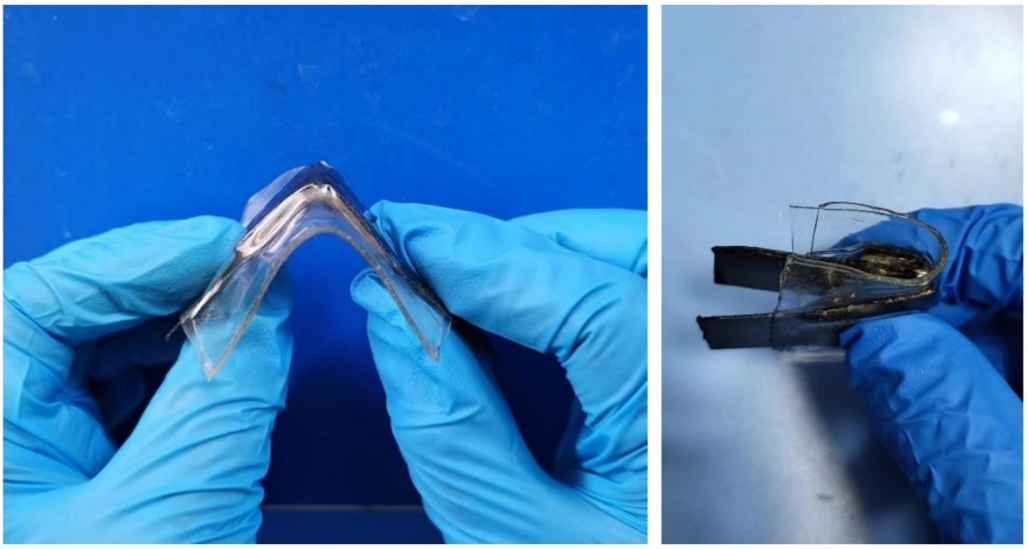

Fig. S11. Digital photo of PHP-10 hydrogel-based FSCs and bending at angle of 90° and 180°.

Reference

1. V. Babel and B. L. Hiran, *Polym Composite*, 2021, **42**, 3142-3157.
2. Y. L. Zou, C. Chen, Y. J. Sun, S. C. Gan, L. B. Dong, J. H. Zhao and J. H. Rong, *Chemical Engineering Journal*, 2021, **418**.
3. J. Du, W. L. Zhu, Q. L. Yang, X. H. She, H. Wu, C. Tsou, D. G. Manuel and H. P. Huang, *Colloid Polym Sci*, 2022, **300**, 111-124.
4. F. L. Lai, Z. M. Fang, L. Cao, W. Li, Z. D. Lin and P. Zhang, *Ionics*, 2020, **26**, 3015-3025.
5. H. C. Jung, R. Vinodh, C. V. V. M. Gopi, M. Yi and H. J. Kim, *Mater Lett*, 2019, **257**.
6. X. Chu, H. C. Huang, H. T. Zhang, H. P. Zhang, B. N. Gu, H. Su, F. Y. Liu, Y. Han, Z. X. Wang, N. J. Chen, C. Yan, W. Deng, W. L. Deng and W. Q. Yang, *Electrochim Acta*, 2019, **301**, 136-144.
7. H. Huang, S. C. Abbas, Q. Deng, Y. Ni, S. Cao and X. Ma, *J Power Sources*, 2021, **498**.